International Journal of Science and Research (IJSR)
ISSN: 2319-7064
Index Copernicus Value (2016): 79.57 | Impact Factor (2017): 7.296

Investigation of Hydrothermal Aquifers under Paka Volcanic Complex in Northern Kenya Rift

Wafula Chembeni Peter[1], Sirma Chebet Ruth[2], Kirui Msk[3]

[1, 2, 3]Department of Physics, Egerton University Njoro Campus P.O. Box 536 - 20155, Egerton, Kenya

Abstract: ***Paka volcanic complex is located in a tectonically active region in northern Kenya rift that is characterized by east-west extensional strain force that exists on the upper crust. The volcano has been covered by most regional geophysical investigations that focused on regional depth analysis*** $> 7\ km$ ***for deeper structural mapping. But regional depth analysis overlooks local depth analysis*** $< 6\ km$***, where key aquifer structural features that are significant have remained relatively poorly constrained. The primary aim of this study was to investigate the hydrothermal aquifers rock hosting system and determining their influence to the recharge of Paka prospect.Our gravity analysis at local depth produced the following results: (1) Bouguer and residual anomaly maps revealed regions of positive and negative gravity anomalies that trends in Northwest direction. (2)The derivative and analytical signal contour maps revealed both deep and shallow high degree of fracturing zones that are of great significance in enhancing fluids permeability and circulations in a hydrothermal aquifers. The deep fractured zones serve as axial and lateral flow paths for recharge of aquifres systems in Paka volcano while the shallow fractured zones direct the flow of meteoric water in the upper parts of the basements into the aquifer system. (3)The shallow hydrothermal aquifer zone occurs at depth 500 m while the deeper hydrothermal aquifer zone occurs at depth 4000 – 5000 m from the earth surface.This aquifer system trends NW – SE that is parallel to the major rift fault and pre-existing Proterozoic regional structures in northern Kenya rift which seems to have played a role in guiding the orientation and trending of aquifer features under Paka volcano. (4) The 3D density model revealed density distribution patterns that are consistent with the existence of several high density rock intrusions and hydrothermal aquifers systems associated with high density fracturing within Paka volcano. It is overlain with a surficial pyroclastic sediments or Paka Basalt (200 – 300) m layer thickness across the volcano of density range (2.00 – 2.60) g/cm^3 that form capping layer for hydrothermal aquifers systems. (5)Negative gravity zones are due to parts of rock fracturing and of density range (1.80 – 2.40) g/cm^3 that is highly porous to allow infiltration of surface meteoric water into shallow and deeper aquifer. Also, provides favorable pathways for hydrothermal fluids flow and deep circulation of fluids. The zones forms a good hydrothermal aquifers system or hosting rock reservoir for the geothermal system.(6)The fractured aquifer zone on the eastern flank of the Paka volcano massif can be a good target for drilling geothermal wells due to active fault zone associated with the largest mass output. Among the many recommendations highlighted, the study recommends an exploratory borehole drilling be undertaken in Paka volcanic area from the caldera summit towards the eastern flank and northwestern flank along the fractured zones F and G.***

Keywords: Paka volcanic complex; hydrothermal aquifers; local depth analysis< 6 km; gravity data; highly fractured zones

1. Highlights

1) Local depth gravity analysis < 5 km it unfolds the near surface overlooked concealed aquifer key structural features that can be used in identifying areas with favorable aquifer systems and guides in geophysical exploration
2) The hydrothermal aquifers under Paka volcano are recharged by both deep and shallow highly fractured fault zones that trend in NW-SE and N-S
3) The deeper fractured parts of rocks or deeper fault zoneforms a good aquifer system or a good hydrothermal rock hosting system
4) Exploratory geothermal borehole drilling be undertaken in Paka volcanic area from the caldera summit towards the eastern flank and northwestern flank along the fractured zones F and G

2. Introduction

Paka volcanic complex is situated in a tectonically active complex region in the northern Kenya rift that is characterized by east-west extensional or trans-extensional strain force that exists on the upper crustal structure. The regional extensional strain force has resulted in the evolution of Kenyan rift that was accompanied with magmatic and tectonic activities of volcanism and faulting where several calderas have been formed in major volcanoes along the rift floor (Dunkley *et al*., 1993). Along the Kenyan rift, the active volcanoes include from the south: Suswa, Longonot, Olkaria, Eburru, Menengai, Arus-Bogoria, Korosi, Chepchuk, Paka, Silali, Emuruangogolak, Namarunu and Barrier volcanic complex (Robertson *et al*., 2016; Waswa, 2017). Paka volcano area is located approximately 25 km north of Lake Baringo and 15 km east of the Nginyang' village at 00° 25' N and 36° 12' E and rises to a maximum altitude of 1697 m. It has an irregular outline covering an area of approximately 280 km² (Dunkley *et al*., 1993; Smith, 1994).

The magmatic activities of Paka volcanic complex commenced during the late Pleistocene (Neogene period 390 Ka to 10Ka) with the intrusion of mafic magma into the shallow chamber. The magma chamber occurs at depth of about 6 km in most of the rift volcanoes (Omenda, 1998; Simiyu and Keller, 2001; Mariita and Keller, 2007). The presence of Quaternary (Neogene) eruptions of young Basalt lavas~ 10 Ka that extends northwards from the caldera to NNE trending fissures (Mutonga, 2013),the occurrence of seismicity events that are observed to the east flank of the Paka volcano (Patlan *et al*., 2017),the Geodetic ~ 21 cm uplift activities that occurred at Paka during the 2006 – 2007 (Biggs *et al*., 2009), and the many surface geothermal expressions that includes teaming ground, fumaroles and hot springs are indicators that Paka magma chamber is still active (Lagat *et al*., 2007; Kanda *et al*., 2011; Mwakirani, 2011). The surface expressions of high-temperature

fumaroles > 97℃ (Omenda, 2014b) and the hot springs are indicators of high permeability under Paka volcano and are tapping deep hydrothermal aquifer fluids. The occurrence of fumaroles are indicators of the presence of concealed or hidden hydrothermal aquifers and faults that transmits fluids into the aquifer as wells as providing paths for upwelling hot aquifer fluids (Omenda, 1998).

Most of the early studies along the axial Kenyan rift focused on analyzing the regional tectonic evolution of Kenya rift, crustal analysis and geothermal energy explorations at regional depth analyses (8 – 40) km. The studies were summarisedin three publications (Prodehl *et al*., 1994, 1997; Morley, 1999a).Many authors have discussed the subject of what controls the older feature exactly on the location of the rift on both local and regional scale, for example, Smith and Morley (1993) suggested that the old regional NNW-trending lineaments, which are associated with the mobile belt control the geometry of Sudan-Anza rift system. At regional view, major boundary fault in the east African rift system tends to transfer displacement along overlapping segments, along which displacement gradually dies out on one fault and increases on one or more others (Smith, 1994). Darling *et al*. (1996) extended the delineation of major rift faults of Smith and Morley (1993) and Smith (1994) to regional fault structural controls on the hydrothermal fluid migration along the East African Rift. The study indicated that there is a northward flow of major lake water with no surface outlets along the axial fault. For example the deep well drilled $\sim 2000m$ at Olkaria and Eburru volcanic fields indicates the deep circulation of Lake Naivasha water, the Perennial hot spring of Kapedo, west Silali volcano have an output comparable in volume to the loss estimated for Lake Baringo water that also applies to the Lorusio hot spring located 10 km to the north of Kapedo. Also, there is a strong evidence that northward flow from Awasa lake in the main Ethiopian rift that is observed outside the Corbetti caldera to the E and NE at the boreholes TG-7 and TG-3 at the north of Koka and the fumarole at Borama. At regional scale analyses, Simiyu and Keller (2001) extended the studies done by Smith (1994), Darling *et al*. (1996)and Morley (1999b) to the southern rift (from Menengai to Lake Magadi) where the study showed that the southern part of the Kenya rift consistently have the major fault along the western boundary of the rift valley, and there was no evidence for half graben polarity reversals for a distance of about 300 km. This southern dealineated fault by Simiyu and Keller (2001) was viewed as a southern axial fault structural controls on hydrothermal fluid deep circulation. Mariita and Keller (2007) extended the study done by Simiyu and Keller (2001) to the northern Kenya rift (from Menengai to Lake Turkana), and he made a similar observation as the one observed in the southern rift.Majorly the study focused on axial rift gravity highs associated with rift volcanoes.

Most of these studies focused on the tectonic evolution of the East Africa rift, crustal analysis and structural fault controls on hydrothermal deep circulation at regional depth analysis (>8 km). The regional depth analysis (>8 km) maps deeper crustal structures associated with low frequency and the long wavelength. However, regional depth analysis (>8 km) overlooks local depth analysis< 7 Km that deals with near surface features associated with high frequencies and short wavelengths which can provide additional information on local depth at the shallow upper crust. In contrast, the local depth analysis < 7 km under Paka volcano which has received little-to-no individual local depth analysis< 7 Km that is significant in the investigation of Paka hydrothermal aquifers have remained relatively poorly constrained despite the many geothermal surface expressions. Hence, the local depth geological features like increased fracture density associated with lower Trachyte's that generates the zones of high permeability, conducive for deep circulation and fluid flow (favorable hydrothermal aquifer structural setting) have not been mapped at regional analysis. To extend the studies carried out at a regional scale in the northern Kenya rift to a detailed local depth analysis in Paka prospect, our study employed gravity inversion modeling, derivative techniques and analytical signal filters at local depth analyses< 6 Km to improve and bring out new information on subsurface favorable aquifer structural setting under the Pakavolcanic architecture with the view to investigate aquifers rock hosting system and determining their influence to the recharge of Paka prospect.

Therefore, understanding the subsurface volcanic architecture is significant to fully explain how the local structurescontrol the hydrothermal fluid movement and its favorable hydrothermal aquifer rock hosting system (Connor *et al*., 2000; Betts *et al*., 2003; Blaikie *et al*., 2014; Miller, 20017). Since the regional analysis was inadequate for elucidating the subsurface aquifer rock hosting system, hence they have remained undetermined favorable aquifer accommodation structural zones where the system resides. But Paka volcano is situated in an active rift where extensional strain force promotes both high heat flow and dilation on normal faults, thus inducing deep circulation of meteoric water, increased rock hosting system and up-flow along the fault zones. Therefore, studies have indicated that closely-spaced fault zone has a capacity to host and control the separate aquifer exploitable hydrothermal system that can rival those regions with higher strain rate (Faulds *et al*., 2010a, 2010b; Faulds and Hinz, 2015). Hence, we hypotheses that hydrothermal aquifer or aquifer rock hosting system is significantly controlled and occurs in belts of intermeshing, overlapping or intersecting faults where extensional setting exist.

Bouguer gravity data were utilized as an economical and quick reconnaissance tool for geophysical imaging and assessment of the subsurface favorable hydrothermal aquifer rock hosting system (Cooper, 2004; Mariita, 2007). The main objective of this study was to investigate the hydrothermal aquifers rock hosting system and determining their influence on the recharge of Paka prospect or Paka volcano from the potential gravity data.The edge enhancement techniques employed in this gravity data analyzing includes horizontal gradient HG, tilt derivative TDR, analytical signal and gravity inversion modeling. The edge enhancement techniques are majorly utilized to delineate discontinuities among different geological bodies of various sizes and depth based on density contrast (Verduzco *et al*., 2004; Cooper and Cowan, 2008, 2011; Ma *et al*., 2015; Narayan *et al*., 2017). The techniques are based on different functions of derivatives and analytical signal that transforms the data in the space domain using Fast

Fourier Transform (FFT). The high-density contrast hydrothermal rock hosting system in a volcanic environment is assumed to be as a result of prominent discontinuities or contrasting subsurface densities (Holden *et al*., 2008; Walia *et al*., 2010; Narayan *et al*., 2017). Combining this technique aims at improving the edge detection and delineating the high-density contrast hydrothermal rock hosting system in a volcanic setting (Ekinei and yigitbas, 2015; Narayan *et al*., 2017).

3. Geology and Tectonics in Paka Volcanic Complex

The evolutionary history of Paka volcano was broadly separated into two periods of trachytic volcanism separated by basaltic activity and faulting. The early history of Paka volcano was uncertain as the older shield forming lavas are mantled by trachytic pyroclastic deposits which covers much of the northern, western and southern flanks of the volcano (Baker and Wohlenberg, 1971; Sceal, 1974; Fairhead, 1976; Smith and Mosley, 1993; Hautot *et al*., 2000). The summit area and the upper flanks of Paka volcano are characterized by the short trachyte flow that can be discerned beneath the mantle of younger pyroclastic deposits. Basalt lavas erupted from fissures and cones located along N-trending fractures on the northern and southern flanks, and contemporaneous normal faulting led to the formation of N-trending linear zone of the rifting that extended down the northern flanks. The rift zones are defined by two faults, the Eastern and Western boundary faults that controlled the dispersion of lava and pyroclastic flows during the final stages of eruption and caldera collapse, and also constrain the geothermal activity of Paka. Trachyte and basalt lavas erupted in the caldera and flowed out through a breach and down the northern flanks (Smith and Mosley, 1993; Prodehl *et al*., 1994, 1997). In the south, at Adomeyan faulted trachyte lavas flows erupted from N-trending fissures zones extending between Paka and Korosi (Smith and Mosley, 1993; Prodehl *et al*., 1994, 1997).

The tectonic of Paka is dominated by a zone of intense normal faulting and fissuring located on the eastern and northeastern flanks. This faulting has down faulted older Pleistocene and Pliocene strata of the rift margin against the younger lavas of Paka, and forms part of a larger belt of deformation which extends northwards onto Silali and southwards to Korosi (Baker and Wohlenberg, 1971; Sceal, 1974; Truckle, 1977; Golden, 1978; Smith and Mosley, 1993). In contrast, there is no evidence for faulting nor fissuring to the west of Paka on the Natan plains. Extensive faulting accompanied by block tilting characterizes the terrain and these form numerous N-S ridges and fault scarps. According to Baker and Wohlenberg (1971), Baker (1986) and Baker *et al*., (1972, 1988), this complex network of faults and fractures suggests that tensional strain oblique to the primary rift axis is still occurring.

Gravity Data

Most of the geophysical information on the tectonic evolution of Kenya rift and geothermal exploration comes from seismic and resistivity studies (Swain *et al*., 1981; Swain, 1992). However, these studies are more expensive to handle, and to some extent, they are limited to topographic and geographic structures (Telford *et al*., 1990; Simiyu and Keller, 1997, 2001; Oldenburg and Pratt, 2007; Girdler, 2013; Kearey *et al*., 2013). Gravity data were preferred at the expense of other geophysical methods since it provides the necessary information and delineating the causative body causing the gravity anomaly variations (Mariita, 2003; Oldenburg and Pratt, 2007; Girdler 2013; Kearey *et al*., 2013; Mulwa & Mariita, 2013, 2015; Maucourant *et al*., 2014; Ochieng, 2014).Also, gravity data are cost-effective means to mapthe high density contrast favorable hydrothermal aquifer rock settings in a volcanic environment where other geophysical data were inadequate for elucidating the rock aquifer hosting system(Simiyu and Keller, 1997; Mariita and Keller, 2007; Mariani *et al*., 2013; Oruc *et al*., 2013). In this study, gravity data were used to investigate the hydrothermal aquifers system in relation to rock fracturing that provides favorable accommodation for hydrothermal fluids at local depth< 6 Km in the Paka prospect. The gravity analyses at local depth aimed at bridging the gaps and providing more detailed information on the hydrothermal aquifers system.

4. Horizontal Gradients (HG)

The methods are extensively used in locating the boundaries of high-density contrast from gravity data (Fedi and Florio, 2001; Anudu *et al*., 2014; Ma *et al*., 2015; Yuan and Yu, 2015). The methods contends that the HG of the gravity anomaly caused by a tubular body, tends to overlie the edges of the body if the edges are vertical and well separated from each other (Cordell and Grauch, 1985; Anudu *et al*., 2014; Ma *et al*., 2015; Yuan and Yu, 2015). Maxima of HG indicate the location of the faults or contacts. The greatest advantage of the HG methods is that it is less susceptible to noise in the data because it requires only the calculation of the two first-order horizontal derivatives of the field. The methods are also more robust in delineating both shallow and deep sources. The amplitude of the HG is expressed as:

$$\mathrm{HG} = \sqrt{\left(\left(\frac{\partial g}{\partial x}\right)^2 + \left(\frac{\partial g}{\partial y}\right)^2\right)}$$

Where g is the gravity field, observes at (x, y), $\frac{\partial g}{\partial x}$ and $\frac{\partial g}{\partial y}$ are the two horizontal derivatives of the gravity field in the x- and y-direction.

5. Tilt Derivative (TDR)

The tilt derivative TDR is also known as a tilt angle method, which is a refinement of the analytic signal method (Verduzco *et al*., 2004; Anudu *et al*., 2014; Ma *et al*., 2015; Yuan and Yu, 2015). The TDR determines the location and depth of vertical magnetic contacts or high density contrast fault zone without the prior information on the source configuration by using the horizontal gradient amplitude (first horizontal derivative) of the tilt angle (Oruc, 2011; Anudu *et al*., 2014; Ma *et al*., 2015; Yuan and Yu, 2015). There is a further development from Salem *et al*., (2007) and Fairhead *et al*., (2008). The TDR method is used to enhance and sharpen the potential field anomalies. The advantage of the method is that it shows the zero contour line located on or close to a fault. The TDR is defined as:

$$TDR = \tan^{-1}\left(\frac{\frac{\partial g}{\partial z}}{\sqrt{\left(\left(\frac{\partial g}{\partial x}\right)^2+\left(\frac{\partial g}{\partial y}\right)^2\right)}}\right)$$

Where g is the gravity field observed at (x, y) and $\frac{\partial g}{\partial x}$, $\frac{\partial g}{\partial y}$ and $\frac{\partial g}{\partial z}$; are the two horizontal and vertical derivatives of the gravity potential field respectively. The derivative is restricted within the range + $\frac{\pi}{2}$ to - $\frac{\pi}{2}$ (Salem *et al*., 2007; Fairhead *et al*., 2008)

6. Analytic Signal (AS)

The analytic signal technique is also known as total gradient method and has been the subject of continuing investigation and improvements since it was first applied (MacLeod *et al*., 1993; Roest *et al*., 1992; Hsu *et al*., 1996; Debeglia and Corpel, 1997; Keating and Pilkington, 2004; Dragomiretskiy and Zosso, 2014; Oruc, 2014; Boashash, 2015). The method assumes that the causative sources are magnetic contact or a region having high-density contrast (fault zones). The general equation for 3D gravity source is defined as:

$$AS\ (x, y) = \sqrt{\left(\left(\frac{\partial g}{\partial x}\right)^2 + \left(\frac{\partial g}{\partial y}\right)^2 + \left(\frac{\partial g}{\partial z}\right)^2\right)}$$

Where $\frac{\partial g}{\partial x}$, $\frac{\partial g}{\partial y}$ and $\frac{\partial g}{\partial z}$ are the two horizontal and vertical derivatives of the gravity respectively. The techniques have an ability to identify regions having high-density contrast. The higher values or maxima of analytic signal amplitudes indicates that the regions have a significant density contrast that produces an identifiable signature on the map (Dragomiretskiy and Zosso, 2014; Boashash, 2015; Yuan and Yu, 2015). The maxima of AS amplitudes produces a clear resolution for the shallower bodies (sources), but it does not delineate deeper bodies very well (Arisoy and Dikmen, 2013). The analytic signature of the Paka prospect was calculated in the frequency domain using the Fast Fourier Transform technique (Blakely, 1995).

7. VOXI Earth Inversion Modeling

VOXI Earth modeling tool in Geosoft Oasis Montaj software is a computer modeling program for gravity data that provides a particularly useful means to model and give a clear picture of the density distribution in the subsurface (Swain, 1994; Roy *et al*., 2017; Richarte *et al*., 2018; Strom, 2018). The software generates 3D voxel models from gravity data using cloud-computing (Longo *et al*., 2016). VOXI session was created by first defining the geographical area of interest (AOI) using a polygon file outlining the distinct region of an anomaly. A digital elevation model (DEM) for the area was also created and entered into the new VOXI session as a grid. The type of the potential field data was also entered,and in this case, residual gravity gird was used. The constraint density for the inversion process was 2.67 g/cm^3. A linear background was not removed since the removal of background can remove some residual data. The inversion process runs online (using the internet) for some minutes, depending on the size of the AOI and the number of constraints being applied. When the inversion process is complete, the model is downloaded and is ready for modeling.

8. Results and Discussion

8.1 Bouguer Anomaly Map

In the first place of this gravity analysis, gravity data underwent standard gravity reductions that include free air correction, Bouguer correction, latitude correction and terrain correction (Hinze *et al*., 2005). Gravity data reduction and terrain corrections require knowledge of the average density of subsurface rocks that constitute the topographic relief of the surveyed area. Obtaining any plausible results for Bouguer anomaly, therefore, depends on the determination of the best average density possible for the rocks in an area of investigation (Simiyu and Keller, 2001). Simiyu and Keller (2001) and Mariita (2003) have used some approaches to determine the terrain density for the southern and northern Kenya rift valley respectively. Based on their results, they have used a density of 2.55 g/cm^3 for Bouguer and terrain corrections. Simiyu and Keller (2001) have, however, noted that use of the traditional Bouguer reduction density (2.67 g/cm^3) would not have any significant effect on the resulting Bouguer anomaly. According to Simiyu and Keller (2001), Hinze (2003), Hinze *et al.* (2005, 2013), Mariita and Keller (2007) and Kearey *et al.* (2013) a density value of 2.67 g/cm^3 is assumed for the surface rocks of the continents that are crystalline and of granitic composition. The density of granitic rocks ranges from 2.5 to 2.8 g/cm^3 with an average value of roughly 2.67 g/cm^3. In this study, raw gravity data for Paka prospect was reduced to Bouguer anomaly using Bouguer density 2.67g/cm^3 and sea level as datum traditionally, then it was adjusted to a common IGSN71 having a gravity value of 9775260.7 in gravity datum before being processed in Geosoft Oasis Montaj software (Simiyu and Keller 2001; Hinze, 2003; Mariita and Keller 2007). Bouguer gravity data was projected at Arc 1960 datum and in the UTM zone 37N using Geosoft Oasis Montaj software.

For shallow upper crustal analysis, a bandpass filter and upward continuation filter is applied to simple Bouguer data (Pawlowski, 1994; Pal, 2009; Kearey *et al*., 2013; Mulwa and Mariita, 2013; Shako and Wamalwa, 2014). The choice of bandpass and upward continuation filters for this study was thrilled from the seismic and electromagnetic studies done by Wamalwa and Serpa, (2013), Omenda (2014), Omenda and Simiyu (2015) and Lichoro *et al.* (2017). The seismic study indicates the existence of local events of a hot body occurring at a depth less than 5 km while Magnetotelluric studies show the existence of a conductor directly under Paka volcano at depth< 5 Km. Also, most of regional studies done along the axial rift indicates that the massive intrusive bodies occurs at depth less 6 km from the earth's surface (Simiyu *et al*., 1995; Simiyu, 1996; Simiyu and Keller, 2001; Mariita and Keller 2007; Lichoro *et al*., 2017; Nyakundi, 2017). In this study, a bandpass of 8 km long wavelength and 1 km short wavelength was subjected first to simple Bouguer data then followed by an upward continuation varying from 1 km to 5 km in constructing Bouguer anomaly maps at different local depths (fig.1).From a series of Bouguer anomaly maps that was constructed, they

showed many classic features at local depth better than previously regional gravity maps. Bouguer anomaly maps revealed regions of positive gravity anomalies and regions of negative gravity anomalies that trend in Northwest in Paka prospect but parallel to major faults trends and pre-existing regional tectonic structures like Nyanza rift (Kavirondo) and Proterozoic basement trends.

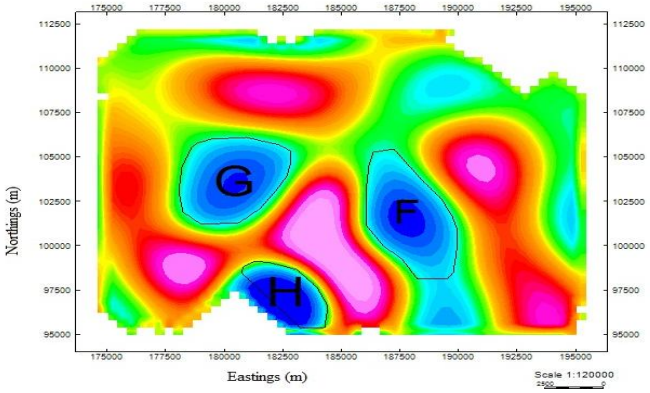

Figure 1: A residual contour map showing the low-density zones encompassed with polygons F, G and H

The positive gravity anomaly signature was due to the high-density intrusion of Trachyte-Basalt rock into the upper shallow crust while negative gravity anomaly signature is due to high-density contrast fracturing of lower Trachyte rock that host and allows both deeper and shallow circulation of hydrothermal fluids.

8.2 Derivative Contour Anomaly Maps

8.2.1. Horizontal Gradient Contour Map

The technique is extensively used to locate the boundaries of density contrast from gravity data. With the aid of Oasis Montaj software, HG filter was subjected to the gravity Bouguer grid to generate a horizontal gradient map (fig. 2). According to Rosid and Siregar (2017), and Cooper and Cowan (2008, 2011) the horizontal derivative can identify or show the existence of near-surface highly fractured zones that is indicated by a zone of highest anomalous gravity value because on the fractured fault zone there is highest contrast rock density. Therefore from figure 2, the region labeled 1, 3 and 5 are near surface highly fractured zones due to the highest anomalous gravity value. Also, deeper the depth of the highly fractured zones can be observed,but the gravity anomalous amplitude value gets smaller (Rosid and Siregar, 2017). In that case, regions labeled 2, 4 and 6was interpreted as deeper highly fractured zones. In another way, the anomalous gravity values on horizontal derivative contour map can be explainedregarding variations of dip normal faults, where the greater dip of the normal fault the bigger amplitude value of horizontal derivative as the gravity horizontally contrast increases. Hence, regions 1, 3 and 5 are viewed as highly fractured zones with greater dip while the regions 2, 4 and 6 are fault zones with less dip. The interpreted faults zones both deep and near-surfacehighly fractured zones trends in Northwest to the southeast direction that is parallel to major rift fault and pre-existing Proterozoic basement regional tectonic structures (Mulwa *et al*., 2014; Wedge *et al*., 2016). Hence, these pre-existing structures seem to have played a role in guiding the orientation of the interpreted highly fractured zones (hydrothermal aquifer systems). But Paka prospect is situated in northern Kenya rift where extensional stretching force (extension local stress regime for shallow magmatism) that was subjected to crustal layer during the rifting process, the weak zone developed half graben or swarms of intra-faults as a result of rock fracturing (Njue, 2015; Robertson *et al*., 2016).The zones of highly fractured can accommodate aquifer and enhances both deeper and shallow circulation of fluids. The maxima of the HG in the horizontal gradient map indicate the location of the hydrothermal aquifer systems.

8.2.2. Tilt Derivative Contour Map (Tilt Depth Map)

The technique was used to enhance and sharpen the gravity potential field anomalies. In Oasis Montaj software, the tilt derivative contour map was mapped through the application of tilt derivative filter on the gravity Bouguer grid (fig. 3). The zero contours in figure 3delineate the edges between two geophysical structures. This geophysical edge structurewas interpreted as fault contact. Also, the depth to the top of the highly fractured zone was estimated directly from the tilt depth contour map figure 3 by simply measuring the distance between appropriate contours of the gravity data that is restricted to the range - 45 °, 0°,and +45°. In Oasis Montaj software has a display method that uses a color contour fill which allows rapid visual inspection of depth variations over a geophysical study area (Fairhead *et al*., 2010). From figure 3, the zero contours occur at depth range (2.5 – 3.0) km that it is the depth to the top of the aquifer system. The fault boundary is in between the high anomalous gravity amplitude associated with shallow massive intrusive (depth less than1.5 km) and the deeper aquifer zones associated with smaller anomalous gravity amplitude at depth 4.5 – 5.0 km. The delineated aquifer systems trends in N-S, E-W, NW-SE,and NE-SW at a different depth from the earth's surface. This favorable aquifer trending structure agrees with Dunkley *et al*. (1993) the topographic fault trending.

8.2.3 An Analytic Signal Contour Map

The analytic signal filter can locate and identify zones of highly rock density contrast at a different depth by producing maxima over the high-density rock contrast regardless of the high-density fracture strikes (MacLeod *et al*., 1993). The maxima amplitude values identified in the analytic signal map in figure 4 delineates a highly permeable aquifer zone. The amplitude gravity values increase with the reduction of depth to the top of the aquifer structure zone. From this augment, the permeable aquifer zone in the region H occur at shallow depth while the favorable aquifer structural sources at NW and NE of Paka prospect occur at deeper depth. The high maxima zones on the Analytic signal contour map was interpreted as zones with a high degree of fracturing. The low-density zones F, G and H from figure 1 that was overlaid on top of the analytic signal map, the regions exactly coincided with the maximum amplitude values of the analytic signal map (fig. 4). The high maxima zones on the Analytic signal contour map was interpreted as zones with a high degree of fracturing. This coincided withlow-density zone on residual anomaly map with maxima regions on analytic contour map implies that the low-density zones are associated with a high degree of fracturing. The fracture zone that runs from the north through G and H can be interpreted as an axial fault zone

while the fault zone from H through F to the northwest was interpreted as a lateral fault that recharges Paka aquifers system.

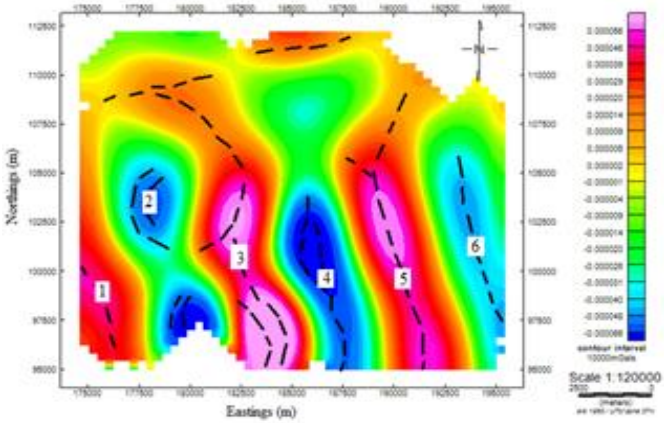

Figure 2: The horizontal gradient contour map that shows a shallow and deeper geophysical aquifer structures

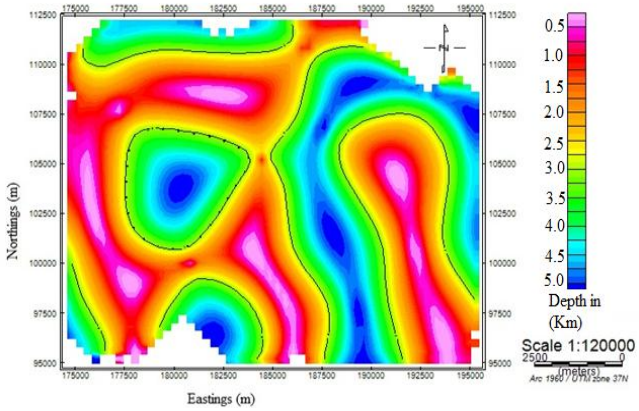

Figure 3: The zero contours on the tilt depth map shows a geophysical aquifer structure

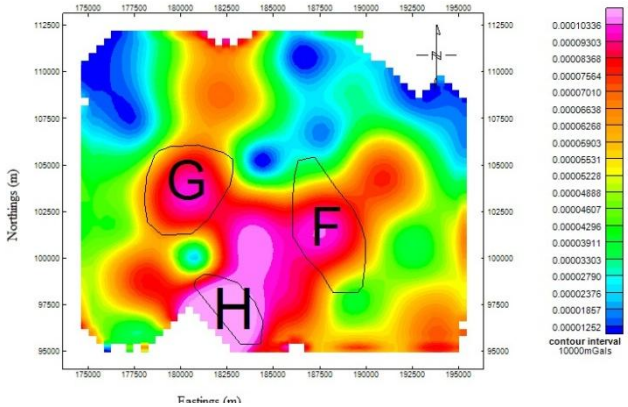

Figure 4: The Analytic signal contour map shows the geophysical aquifer structure zones

8.3 Inversion Modeling

8.3.1 An Inversion Model for Region F (*Eastern Flank of Paka Summit*)

An inversion under region F from figure 1 was aided via VOXI earth modeling tool in Geosoft Oasis Montaj. The region covered an area of 19.17 km^2 and the inversion process processed in 16 grid block cells in the x-direction and 30 grid block cells in the y-direction and 14 grid block cells in a z-direction. Initial model had a density range of (2.528 – 2.697) g/cm^3 and extended to a maximum depth of 2351 m from the earth's surface. The inversion process subjected to gravity 'low' under region F from figure 1, was achieved by removing the high-density material from the initial model. On modeling to a depth of 408 m from the earth's surface, the density range was (2.528 – 2.682) g/cm^3 (fig. 5). Further removal of high density from the model to the density range of (2.528 – 2.616) g/cm^3, the depth to the top model increased to 938 m from the earth's surface.

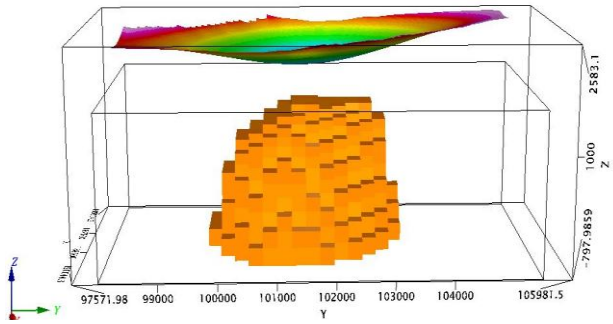

Figure 5: Aninversion model for region F at density range (2.528 – 2.682) g/cm^3

Under region F, the surficial layer is characterized with high density above 2.620 g/cm^3 at a depth 600 m; itwas tentatively interpreted as volcanoclastic / pyroclastic sediments that forms a capping that overlain a lower density aquifer zone. As depth increases from 600 m to 2351 m from the earth's surface, the density reduces approaching 2.528 g/cm^3. This low-density rock structurewas interpreted as due to higher porosity or highly fractured parts of rocks. Due to higher porosity or highly fractured parts of rocks, the zone provides a good structural setting that allows recharge of the prospect and penetration of meteoric water into deep crust towards the high density/hot magmatic modeled bodies. According to Swain (1992), Mariita and Keller (2007) and Sippel *et al.* (2017) the density of the host rock is taken as 2.70 g/cm^{3}and a density range of (1.60 – 2.70) g/cm^3 has been augmented as density for gravity 'low'. The low-density aquifer structures trends in NW – SE. But according to Robertson *et al.* (2016) and Wedge *et al.* (2016), the pre-existing Proterozoic basement trends in NW-SE and the presence of extensional local stress regime in northern Kenya rift, seem to control this aquifer orientation under region F.

8.3.2 An Inversion Model for Region G (*South Riongo Area*)

Region G from figure 1 covers an area approximate 18.10 km^2, and inversion was aided using VOXI modeling tool in Geosoft in Oasis Montaj. The model was generated using 20 grid block cells in the x-direction and 21 grid block cells in the y-direction and 13 grid block cells in the z-direction. An initial model had a density range (2.00 – 2.632) g/cm^3, and the model extends to a maximum depth of 2085 m from the earth's surface. The high-density material was clipped out of the model since the inversion was for low gravity region. At density range (2.00 – 2.548) g/cm^3, the depth to the top of the model was 534 m from the ground surface. On further removal of high-density material from the model to depth 1174 m, density changed to (2.00 – 2.417) g/cm^3 (fig. 6).The surficial high-density layer more than 2.60 g/cm^3 that overlain the low-density zone was due to volcanoclastic / pyroclastic sediments. This surficial high-density layer

seems to provide the capping to the low-density zone. Reduction in rock density as depth increases might be due to high porosity or fracturing of rocks. Tentatively at the depth greater than 1174 m, the zone was interpreted as altered clay zone based on Kearey *et al.* (2013) since clay minerals are majorly associated with hydrothermal aquifers system, the density of clay is (1.63 – 2.60) g/cm^3.Tentatively at the depth greater than 1174 m, the zone was interpreted as altered clay zone based on Kearey *et al.* (2013) since clay minerals are majorly associated with hydrothermal aquifers system and the density of clay is (1.63 – 2.60) g/cm^3.

8.3.3 Gravity Inversion Model for Region H (*Southern Flank of Paka Summit Area*)

The region covers an area approximate7.73 km^2 and inversion model was generated with 16 grid block cells in the x-direction and 16 grid block cells in the y-direction and nine grid block cells in the z-direction. An initial model had density range (2.281 – 2.672) g/cm^3 and it extends to a maximum depth of 1454 m from the earth's surface. On modeling to a density range (2.281 – 2.658) g/cm^3, the depth to the top of the model was 720 m (fig. 7). Furthermodeling by clipping out the high-density material from the model a depth 905 m, the density change to (2.281 – 2.505) g/cm^3.According to the Kearey *et al.* (2013) and Nyakundi (2017), the calculated density ranges for

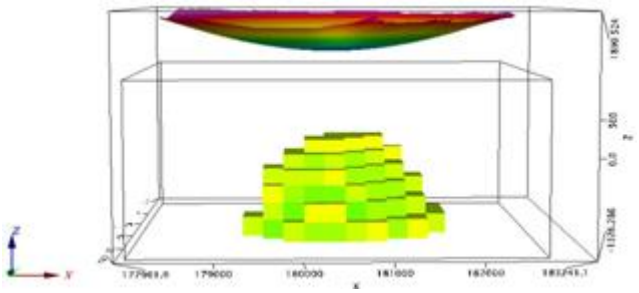

Figure 6: Inversion Model at Density Range (2.00 – 2.417) g/cm^3

this region falls under the gravity 'low' of density range (1.60 – 2.70) g/cm^3. The high-density surficial layer greater than 2.60 g/cm^3 was due to volcanoclastic sediments that form a cap to the lower density zone. As depth increases, the density approaches 2.281 g/cm^3 for region H that was interpreted as a zone of high porosity or highly fracturing. As per Lichoro *et al.* (2017), the zone of high porosity or highly fracturing was viewed as hydrothermally altered clay zone.

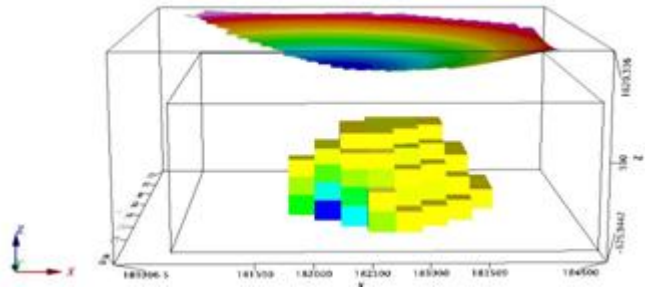

Figure 7: An inversion for region H at density range (2.281 – 2.658) g/cm^3

8.4 The 3D Density Model of Paka Prospect

An inversion model for Paka prospect that covers 258.49 km^2 was constructed using the VOXI earth modeling tool in Geosoft Oasis Montaj. The model had initial density range (1.84 – 3.181) g/cm^3 at maximum extends 4608 m from the earth's surface. The inversion model of Paka area was converted into a 3D density model using an export tool in models manager of Geosoft in Oasis Montaj version 8.5 (fig.8). The 3D density model revealed a density distribution patterns that are consistent with the existence of the several hydrothermal aquifers system within the Paka prospect. The subsurface local depth geology was explained regarding the 3D density model and interpretations based on Simiyu and Keller (2000, 2001).

Paka prospect is overlain with the surficial layer of density range (2.00 – 2.60) g/cm^3 volcanic soils and sediments at thickness 200 – 300 m. The surficial layer density it is in line with Arus-Bogoria modeled 2.40 g/cm^3 surficial density (Mulwa and Mariita, 2013).

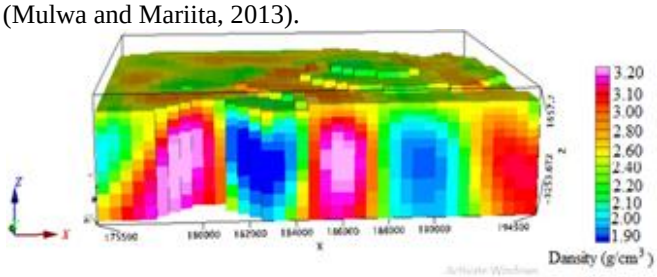

Figure 8: The 3D density model of Paka prospect

Vertical planes across the density model along y-direction were employed to analyze vertical density variations. A profile 99000 northings figure 9 indicates vertical density variations intrusive structures. West of region D has a slanting low-density material less than 2.60 g/cm^3 that was interpreted as volcanic sediments or due to highly fractured parts of rocks. Region D and C is overlain with (2.00 – 2.60) g/cm^3 low-density volcanic soils and sediments. At a depth, more than 400 m from the earth's surface, the density for regions C and D increases from 2.60 g/cm^3 to 3.20 g/cm^3 that was interpreted as dike intrusion or shallow magma. For region F, its density is less than 2.20 g/cm^3 at depth more than 4608 m maximum extents. Due to (1.90 – 2.30) g/cm^3 low density in zone F, then the zone F was interpreted as a result of volcanic soils or highly fractured rocks. Region B has a density (2.40 – 3.10) g/cm^3 that was interpreted as a high-density intrusion dike bordering (2.10 – 2.40) g/cm^3 fractured rocks on either side.

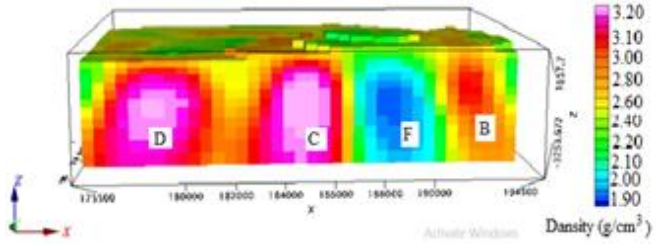

Figure 9: Profile 99000 in the y-direction across the 3D density model

From figure 10 it means that the right triangular region B intrusion trends in NW – SE direction. The rock density (1.60 – 1.90) g/cm^3 for region G increases while region F

reduces (fig.10), but rock fracturing is well developed at its center. The rock fracturing that is well developed for region G downwards has greatly affected the roots for the high-density intrusion of E and C (fig.10). The low density for region G that is as a result of intensely fracturing/faulting can form a good reservoir rock for geothermal fluids (hydrothermal aquifer).

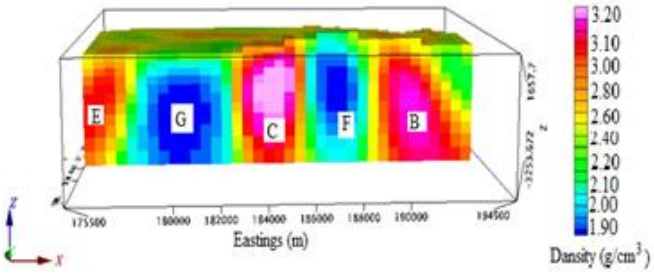

Figure 10: Profile 102700 in the y-direction across the 3D density model

Generally, the calculated surficial layer low density (2.10-2.60) g/cm^3 agrees with the Mulwa and Mariita (2013) modeledlow surficial density of 2.4g/cm^3 due to volcanic soils sediments at Arus-Bogoria in the south of Paka prospect. According to Kearey *et al.* (2013) and Nyakundi (2017), an intruding rock has a density ranging from (2.70 – 3.20) g/cm^3. From our interpretation of high-density intrusions, then it agrees with Kearey *et al.* (2013), and Nyakundi (2017) augments and for the low-density zones. Comparing the (2.60 – 3.20) g/cm^3 calculated modeled high-density intrusion and the axial rift profile gravity high model mafic body of density 2.9 g/cm^3 by Simiyu and Keller (2001), then it agrees with it. All modeled high-density intrusion and the low-density zones trends in NW – SE. But according to Mutonga (2013) and Wedge *et al.* (2016), the Proterozoic basement trends in NW – SE in northern Kenya rift (from Menengai towards Lake Turkana). Hence, from this study, the Proterozoic basement seems to have played a role in guiding the magmatic dike intrusions and low-density zones (hydrothermal aquifer orientation in Paka prospect.

9. Discussion for the Results

Kenyan rift is under the East African Rift System (EARS), which is an example of an active continental rift zone with its arm extending from southern Ethiopia through central Kenya into Tanzania (Dunkley *et al*., 1993; Smith, 1994). The Kenyanrift encompasses several active volcanoes that include Paka volcano that has undergone immense tectonic activities of volcanism and faulting that formed a caldera at its summit (Mutonga, 2013; Waswa, 2017).

From a series of Bouguer anomaly maps and residual maps that was constructed (fig.1), they showed many classic features at local depth $< 5\,km$better than previously regional gravity maps. Residual anomaly maps revealed regions of positive gravity anomalies and regions of negative gravity anomalies that trends in Northwest in Paka prospect but parallel to major faults trends and pre-existing regional tectonic structures like Nyanza rift (Kavirondo) and Proterozoic basement trends (Smith, 1994; Robertson *et al*., 2016). The positive gravity anomaly signature was due to high density intrusion of Trachyte-Basalt rock into upper shallow crust. Since Paka volcano is dominantly composed of trachytic and basaltic lavas and pyroclastic deposits (Dunkley *et al*., 1993). While negative gravity anomaly signature is due to high density contrast fracturing of lower Trachyte rock that can host and allows both deeper and shallow circulation of hydrothermal fluids. Studies done by Yang *et al*. (1998), Suzuki *et al*. (2001), Faulds and Hinz (2015), and Njue (2015), indicates that the high degree of fracturing of oldest rock that has been overlain by capping rocks forms a good aquifer reservoir rocks for a hydrothermal system. This argument supports our views over a highly fractured lower Trachyte rock as a good aquifer hosting rock structures.

The horizontal derivative contour map highlighted both shallower and deeper highly fractured zones since the techniques generate minimum and maximum gravity anomaly signature over the zones with high contrast rock density at different depths (Cooper and Cowan, 2008, 2011; Kearey *et al*., 2013; Rosid and Siregar, 2017). The near surface or shallow highly fractured zones labeled1, 3 and 5 were indicated by maximum amplitudes (anomaly signatures) on the horizontal derivative contour map (fig. 2). This shallow highly fractured zones could also be explainedregarding greater dipping fractured zones. While the deeper fractured hydrothermal aquifer zones under regions 2, 4 and 6were associated with the fewer fractures dipping zones. The interpreted hydrothermal aquifer zones at deeper and near-surfaceassociated structural structures trends in Northwest to the southeast direction thatis parallel to major rift fault and pre-existing Proterozoic basement regional tectonic structures (Smith, 1994; Mulwa *et al*., 2014;Wedge *et al*., 2016). Hence, these pre-existing structures seem to have played a role in guiding the orientation of the interpreted hydrothermal aquifer system. But Paka prospect is situated in northern Kenya rift where extensional stretching force (extension local stress regime for shallow magmatism) that was subjected to crustal layer during the rifting process, the weak zone developed half graben or swarms of intra-faults as a result of rock fracturing which provided the favorable structural setting for hydrothermal aquifer accommodation (Tapponnier and Molnar, 1977; Alexander *et al*., 2011; Njue, 2015; Robertson *et al*., 2016; Wrage *et al*., 2017).

The zero contours in tilt depth contour map figure 3delineate the edges between two geophysical structures. This geophysical edge structurewas interpreted as fault contact. The depth to the top of highly fractured zones (hydrothermal aquifer system) was estimated directly from the tilt depth contour map figure 3 by simply measuring the distance between appropriate contours of the gravity data that is restricted to the range - 45 °, 0° and +45° (Fairhead *et al*., 2010). In Oasis Montaj software has a display method that uses a color contour fill which allows rapid visual inspection of depth variations over a geophysical study area (Fairhead *et al*., 2010; Vaish and Pal, 2015). From figure 3, the zero contours occur at depth range (2.5 – 3.0) km that it is the depth to the hydrothermal aquifer system. The fault boundary is in between the high anomalous gravity amplitude associated with shallow massive intrusive (depth less than1.5 km) and the deeper structures associated with smaller anomalous gravity amplitude at depth 4.5 – 5.0 km. The depth to the zero contour is in agreement with deep

drilled wells in Olkaria and Eburru at ~ 2000 *m* deep that indicated a significant passage or northward flow of Lake Naivasha water along the major axial highly fractured rift fault zone (Darling *et al*., 1996). The interpreted favorable aquifer structural setting trends in N-S, E-W, NW-SE, and NE-SW at a different depth from the earth's surface. The subsurface favorable aquifer structures trending agrees with Dunkley *et al*. (1993) the topographic fault trending in northern Kenya Rift. The coincident of Dunkley *et al*. (1993) topographic faults and the favorable aquifer structures promotes the downward flow of meteoric water to the aquifer system. The trending structures was also compared with N-S and NW-SE trending faults in Olkaria geothermal field in southern Kenya rift where the faults are characterized by wells that have high Chlorine contents, high temperature and good geothermal producers (Wamalwa *et al*., 2016). According to Wamalwa *et al*. (2016), the NW-SE trending fault in Olkaria is associated with the development of the rift and the pre-existing regional tectonic basement structures that are thought to have played a role in controlling the shallow fault structures. Relating to the trending faults in Olkaria geothermal field, we can conclude that the regional tectonic Proterozoic basement structures might have played a role in guiding the orientation of the interpreted shallow hydrothermal aquifers in Paka volcanic complex in northern rift.

The analytic signal filter can locate and identify zones of high rock density contrast at a different depth by producing maxima over the high-density rock contrast regardless of the fractured density strike (MacLeod *et al*., 1993). The maxima amplitude values identified in the analytic signal map in figure 4 delineates a high-density fracture zone. The amplitude gravity values increase with the reduction of depth to the top of a fault structure or aquifer structure (MacLeod *et al*., 1993). From this augment, the highly fractured zone in the region H occur at shallow depth while the structural sources at NW and NE of Paka prospect occur at deeper depth. The high maxima zones on the Analytic signal contour map was interpreted as zones with a high degree of fracturing. The low-density zones F, G and H from figure 1that was overlaid on top of the analytic signal map; the regions exactly coincided with the maximum amplitude values of the analytic signal map (fig. 4). This coincided withlow-density zones on the Bouguer anomaly map with maxima regions on analytic contour map implies that the low-density zones are associated with a high degree of fracturing. Due to the high degree of fracturing and underlined massive intrusion of hot rocks, the zone can be a good reservoir rock for the hydrothermal aquifer system (Yang *et al*., 1998; Hutchison *et al*., 2015; Njue, 2015; Wilks*et al*., 2017).The low-density zones F, G and H from figure 1 has been interconnected under the analytical signal map (fig. 4). This implies that as depth increases from near surface to approximately 3-5 km deep, the degree of fracturing increase with an increase in depth as indicated in figure 4. But at such deeper depth of 3-5 km, there exist a highly fractured older Trachytic rocks which resulted from a tectonically active region in the northern Kenya rift that was characterized by east-west extensional or trans-extensional strain force that existed on the upper crustal structure during the rifting process (Smith, 1994; Robertson *et al*., 2016; Waswa, 2017). The higher degree of older rock fracturing was interpreted as a favorable hosting zone for hydrothermal aquifer system. The fault zone that runs from the north through G and H can be interpreted as an axial highly fractured fault zone while the fractured zone from H through F to the northwest was interpreted as a lateral fractured fault. The mapped axial fractured fault zone that runs in the western part of a caldera is similar to the Simiyu and Keller (2001) who extended the studies done by Smith (1994) and Morley (1999) to the southern rift (from Menengai to Lake Magadi) where the study indicated that the southern part of the Kenya rift consistently has the major fault along the western boundary of the rift valley, and there was no evidence for half graben polarity reversals for a distance of about 300 km. The axial fault zone and lateral fault zone form a good deeper flow path for the prospect and can be an axial and lateral recharge for the hydrothermal aquifer system under Paka volcano (Darling *et al*., 1996; Lagat *et al*., 2007).

The modeled low gravity zone under regions F – H, from figure 1 was mainly interpreted as due to a highly fractured zone or partial rock melting. But Paka prospect is situated in northern Kenya rift where extensional or stretching force (extension local stress regime for shallow magmatism) that was subjected to crustal layer during the rifting process, the weak zone developed half graben or swarms of intra-faults as a result of increased rock fracturing (Njue, 2015; Robertson *et al*., 2016). From figure (5 – 7), the density decreases with increase in depth from the earth's surface. Therefore as depth increases, the degree of fracturing or rock porosity increases (fig 5 – 7). We interpreted the intensely fractured zone at deeper depth as due to lower trachyte fractured zone since the prospect is dominated by trachyte volcanism that erupted during the late Pleistocene (Omenda, 1998; Mutonga, 2013; Waswa, 2017). This lower trachyte that is highly fractured or faulted can form a good reservoir rock or be a good hosting system for hydrothermal aquifers. The porous and permeable host rocks can promote the hydrothermal fluids circulation to circulate upward and outwards from an underlined igneous Trachytic-Basaltic heat intrusive source at depths. Since from analogous of boiling water from a pot, the hottest water rises fastest directly above the heat source and at the surface change direction of flow to horizontal and finally downwards along the sides of the pot (Lagat, 2007). For the case geothermal boreholes drilling, if drilled in this zones that have favorable aquifer structural setting, then the borehole significantly will have a larger output masses (Simiyu and Keller, 2000; Owen *et al*., 2015).This zone occurs at a depth 1 – 5 km, and if filled with clay minerals due to infiltration, then it becomes a good conductor zone. According to Lichoro *et al.* (2017), from MT and TEM joint inversion, ≈ 10 Ωm low resistive zone interpreted as altered clay zone or due to partial melts of rocks at 1 – 3 km depth coincides with our lower trachyte fractured zone that is viewed as a good rock hosting reservoir. From the analytical signal map figure 4, it is observed that the low density fractured zones regions F – H which is viewed as a hydrothermal aquifers are located on the major deep axial fractured rift faults that provide convective or northwards axial flow from Lake Baringo towards Lorusio hot spring that is 10 km to the north of Kapendo (Darling *et al*., 1996). This axial northward flow of Lake Baringo fresh water can be viewed as a recharge for

the interpreted hydrothermal aquifers (fractured zones under regions F – H) in Paka volcano.

The 3D density model revealed a density pattern consistent with the existence of several high-density rock intrusions and hydrothermal aquifers systems within Paka prospect (fig. 8 – 10). Paka prospect is overlain with the surficial layer of density range (2.10 – 2.60) g/cm^3 volcanic or pyroclastic soils and sediments of thickness 200 – 300 m. The presence of pyroclastic volcanic soils shows the presence of volcanic activities which deposited high materials close to the surface. The pyroclastic layer or the recently eruption of young Basaltic lava $\sim 10\ ka$ (Mutonga, 2013) that cover most of Paka volcano, conceal key features of great significance to the favorable structural hydrothermal aquifers systems like concealed faults that can transmit meteoric cool fluids into aquifer and as well as providing paths for upwelling hot reservoir fluids. The overlain layers of pyroclastic or of young Basaltic lava are of great importance by providing capping layer to hydrothermal aquifer systems or hosting rock reservoirs. The interpreted surficial layer density it is in line with Arus-Bogoria modeled 2.40 g/cm^3 surficial density (Mulwa and Mariita, 2013). Vertical planes across the density model were employed to give more information on density variation at depth. From several profiles developed across the density model, the densities for different structural features were analyzed in details (fig 8 – 10). Intruding rocks of density greater 2.70 g/cm^3 and low-density zones less than 2.60 g/cm^{3}were easily discerned from profiles. The high-density intrusion was due to massive Trachyte-Basalt rock since the prospect is dominated by trachytic and basaltic quaternary (Neogene eruption) eruptions (Mutonga, 2013; Waswa, 2017). On the other hand, the low-density discerned as region F, G and H figure (8 – 10) occur at a depth which does not exceed 5 km. The zone is viewed as due to highly fractured parts of rocks that forms a good hosting rock hydrothermal reservoir system. The zones F, G and H were interpreted as hydrothermal aquifer systems since they are located in zones of a high degree of fracturing and with well existence fractured fault network. The depth to the aquifer systems ranges from 400m to approximately 5 km from the earth's surface. Since Paka volcano is prone to underlined massive intrusions of hot Trachyte-Basaltic rocks, then at a higher temperature more than 800 ℃, the deformation mode on Basalt rocks becomes macroscopically ductile i.e. the deformation is distributed throughout the Basalt rock sample resulting in increased compactness thus porosity and permeability reduces from 7 km downward (Violay *et al*., 2015). The brittle to ductile transition for Trachyte-Basalt bedrock provide a holding capacity of hydrothermal aquifers systems above it and also enhance fluids circulation in the upper zone$< 6\ km$.

The seismicity study done by Patlan *et al.*(2017) indicates a low shear wave velocity anomaly to the east flank of Paka volcanic center at a depth 3 – 6 km that is due to a hot deep fluid to shallow circulation. This study agrees with our interpretation of low-density zone F that occurs at depth 3 km. The highly fractured zone at zone F is sandwiched between hot massive, intrusive B and C that superheat the deep and shallow circulating water (fig 9 – 10). But most seismic studies have shown that massive intrusions are associated with high level of seismicity events. This seismicity event occurs in an active fault associated with fluid movement in a geothermal field (Simiyu and Keller, 2000). From our interpretation, Patlan *et al.*(2017) and Simiyu and Keller (2000) augments, then we concluded that fractured zone at F is an active seismic zone. The highly fractured rocks at zone F can be a good conduit for heat and geothermal fluid movement within the reservoir or within hydrothermal aquifers systems. This zone can be a good target for drilling geothermal wells since such zones have the largest mass output (Simiyu and Keller, 2000; Njue, 2015). But the study done by Sippel *et al.* (2017) indicates that gravity 'low' in the northern Kenya rift including Paka prospect is due to positive thermal anomalies within the crust which involves partial melting or rock expansion that strongly weakens the upper crust.

10. The Conclusion from the Results

The main objective of this research was to investigate the hydrothermal aquifers rock hosting system and determining their influence on the recharge of Paka prospect

10.1 Conclusion Based on Residual Anomaly Map

Residual anomaly maps revealed regions of positive gravity anomalies and regions of negative gravity anomalies that trend in Northwest in Paka prospect but parallel to major faults trends and pre-existing regional tectonic structures like Nyanza rift (Kavirondo) and Proterozoic basement trends. The positive gravity anomaly signature isdue to the high-density intrusion of Trachyte-Basalt rock into upper shallow crust. While negative gravity anomaly signature is due to high-density contrast fracturing of lower Trachyte rock that can host hydrothermal aquifer.

10.2 Conclusion on the Derivative and Analytical Signal Contour Map

From the anomaly contour maps of Paka volcano the study revealed:

i) Both deep and shallow subsurface high degree of fracturing zones those are of great significance in enhancing fluids permeability and circulations in hydrothermal aquifers. The deep fractured zones serve as axial and lateral flow paths for recharge of aquifers systems in Paka volcano while the shallow fractured zones direct the flow of meteoric water in the upper parts of the basements into the aquifer system.
ii) The shallow hydrothermal aquifer zone occurs at depth 500 m while the deeper hydrothermal aquiferzone occurs at depth 4000 – 5000 m from the earth surface.
iii) There is NW – SE trending aquifer structural features that are parallel to the major rift fault and pre-existing Proterozoic regional structures in northern Kenya rift which seems to have played a role in guiding the orientation and trending of aquifer key features under Paka volcano.

10.3 Conclusion Based on Inversion Modeling and 3D Density Models

The following conclusions were derived from an inversion modeling and 3D density model:

1) It revealed a density distribution patterns that are consistent with the existence of several high-density rock intrusions and hydrothermal aquifers systems associated with high-density contrast fracturing within Paka volcano.
2) It is overlain with surficial pyroclastic sediment or Paka Basaltic rocks(200 – 300) m layer thickness across the volcano of density range (2.00 – 2.60) g/cm^3 that form capping layer for hydrothermal aquifers systems.
3) Negative gravity zones are due to parts of rock fracturing and of density range (1.80 – 2.40) g/cm^{3}that is highly porous to allow infiltration of surface meteoric surface water into shallow and deeper aquifer. The zones form a good hydrothermal aquifers system or hosting rock reservoir for the geothermal system.
4) The fractured aquifer zone on the eastern flank of the Paka volcano massif can be a good target for drilling geothermal wells due to active fractured fault zone associated with the largest mass output.
5) The aquifer systems under Paka volcano are recharged by both axial and lateral highly fractured fault zones that forma good deeper flowpath i.e. the northward flow from Lake Baringo fresh water.
6) The older highly fractured Trachyte rocks providea favorable pathway for hydrothermal fluids flow and deep circulation of fluids

11. Recommendations

11.1 Recommendations Based on this Research Results

Following the research results obtained in this geophysical research work, we recommend the following:

i) Local depth gravity analysis < 5 km it unfolds the near surface overlooked concealed aquifer key features that can be used in identifying the area with the favorable setting to aquifer systems and guides in the exploration for such areas.
ii) The hydrothermal aquifers under Paka volcano are recharged by both deep and shallow highly fractured fault zones that trend in NW-SE
iii) The deeper fractured parts of rocks or deeper fault zone, form a good aquifer system or a good hydrothermal hosting system
iv) Exploratory geothermal borehole drilling be undertaken in Paka volcanic area from the caldera summit towards the eastern flank and northwestern flank along the fractured zones F and G

11.2 Recommendations for Future Studies

Even though the volcano area is prone to highly fractured fault zones architecture, microgravity, Magnetotelluric, and microseismic monitoring be undertaken, and more boreholes should be sunk along the highly fractured fault zones to monitor the groundwater flow patterns continuously. Such data could, in turn, play an important role in predicting the future drilling sites.

12. Acknowledgments

We would like to acknowledge the help and input provided by Bridgit Nyongesa; Gichira, and Ndongoli. We are grateful for the Geosoft team for providing us with the Geosoft Oasis Montaj Educational software. We also thank the Ministry of Energy for providing gravity data especially GDC.

References

[1] Alexander, K. B., Ussher, G., & Merz, S. K. (2011). Geothermal Resource Assessment for Mt. Longonot, Central Rift Valley, Kenya. *Geothermal Resources Council Transactions*, **35**, 1147-1154.
[2] Anudu, G. K., Stephenson, R. A., & Macdonald, D. I. (2014). Using high-resolution aeromagnetic data to recognize and map intra-sedimentary, volcanic rocks and geological structures across the Cretaceous middle Benue Trough, Nigeria. *Journal of African Earth Sciences*, **99**, 625-636.
[3] Arisoy, M.O., and U. Dikmen (2013), Edge detection of magnetic sources using an enhanced total horizontal derivative of the tilt angle, *Bull. Earth Sci. Appl. Res. Cent. Hacet. Univ.* **34**(1), 73-82
[4] Baker, B. H., (1986), Tectonics and volcanism of the southern Kenya rift valley and its influence on sedimentation in the African rifts, *Geological Society of London*, **25**, 45-57
[5] Baker, B. H., Mitchell, J.G., Williams, L.A.J., (1988), Stratigraphy, geochronology and volcano-tectonic evolution of the Kedong-Naivasha-Kinangop region, Gregory rift valley, Kenya, *Geological Society of London*, **145**, 107-116
[6] Baker, B.H. and Wohlenberg, J., (1971), Structural and evolution of the Kenya rift valley, *Nature*, **229**, 538-542
[7] Baker, B.H., Mohr, P.A., Williams, L.A.J., (1972), Geology of the eastern rift system of Africa, *Geological Society of America*,**136**, 1-67
[8] Betts, P. G., Valenta, R. K., & Finlay, J. (2003). Evolution of the Mount Woods Inlier, northern Gawler Craton, Southern Australia: an integrated structural and aeromagnetic analysis. *Tectonophysics*, **366** (1), 83-111.
[9] Biggs, J., Anthony, E. Y., &Ebinger, C. J. (2009). Multiple inflation and deflation events at Kenyan volcanoes, East African Rift. *Geology*, **37**(11), 979-982.
[10] Blaikie, T. N., Ailleres, L., Betts, P. G., & Cas, R. A. F. (2014). Interpreting subsurface volcanic structures using geologically constrained 3-D gravity inversions: examples of maar-diatremes, Newer Volcanics Province, southeastern Australia. *Journal of Geophysical Research: Solid Earth*, **119**(4), 3857-3878.
[11] Blakely, R.J. (1995), *Potential Theory in Gravity and Magnetic Applications*, Cambridge University Press, Cambridge, 441 pp.

[12] Boashash, B. (2015). *Time-frequency signal analysis and processing: a comprehensive reference*. Academic Press.
[13] Connor, C. B., Conway, F. M., & Sigurdsson, H. (2000). Basaltic volcanic fields. *Encyclopedia of volcanoes*, 331-343.
[14] Cooper, G. R. J. (2004). The textural analysis of gravity data using co-occurrence matrices. *Computers & Geosciences*, **30**(1), 107-115.
[15] Cooper, G. R. J., & Cowan, D. R. (2008). Edge enhancement of potential-field data using normalized statistics: Geophysics, **73**, *H1–H4. doi: http://dx. doi. Org/10.1190/1.2837309*.
[16] Cooper, G. R. J., & Cowan, D. R. (2011). A generalized derivative operator for potential field data. *Geophysical Prospecting*, **59**(1), 188-194.
[17] Cordell, L., & Grauch, V. J. S. (1985). Mapping basement magnetization zones from aeromagnetic data in the San Juan Basin, New Mexico, The Utility of Regional Gravity and Magnetic Anomaly Maps WJ Hinze, 181–197. *Society of Exploration Geophysicists, Tulsa, Okla*.
[18] Darling, W. G., Gizaw, B., &Arusei, M. K. (1996). Lake-groundwater relationships and fluid-rock interaction in the East African Rift Valley: isotopic evidence. *Journal of African Earth Sciences*, **22**(4), 423-431.
[19] Debeglia, N., and J. Corpel (1997), Automatic 3-D interpretation of potential field data using analytic signal derivatives, *Geophysics*,**62** (1), 87-96
[20] Dragomiretskiy, K., & Zosso, D. (2014). Variational mode decomposition. *IEEE transactions on signal processing*, **62** (3), 531-544
[21] Dunkley P. N., M. Smith, D.J. Allen, and W.G. Darling, (1993). The geothermal activity and geology of the northern sector of the Kenya Rift Valley, *British Geological Survey Research Report SC*, **93 (**1)
[22] Ekinci, Y. L., &Yiğitbaş, E. (2015). Interpretation of gravity anomalies to delineate some structural features of Bigaand Gelibolu peninsulas, and their surroundings (north-west Turkey). *GeodinamicaActa*, **27** (4), 300-319.
[23] Fairhead, J. D., Salem, A., & Blakely, R. J. (2010, April). Continental to Basin-Scale Mapping of Basement Depth and Structure Using the Tilt-depth Method. In *EGM 2010 International Workshop*.
[24] Fairhead, J. D., Salem, A., Williams, S., & Samson, E. (2008). Magnetic interpretation made easy: The tilt-depth-dip-Δk method. In *SEG Technical Program Expanded Abstracts, 2008* (pp. 779-783). Society of Exploration Geophysicists.
[25] Fairhead, J.D., (1976), The structure of the lithosphere beneath the eastern rift, East Africa, deduced from gravity studies, *Tectonophysics*, **30**, 269-298
[26] Faulds, J. E., &Hinz, N. H. (2015, April). Favorable tectonic and structural settings of geothermal systems in the Great Basin region, western USA: Proxies for discovering blind geothermal systems. In *Proceedings of the World Geothermal Congress, Melbourne, Australia* (pp. 19-25).
[27] Faulds, J. E., Coolbaugh, M. F., Benoit, D., Oppliger, G., Perkins, M., Moeck, I., &Drakos, P. (2010a). Structural controls of geothermal activity in the northern Hot Springs Mountains, western Nevada: The tale of three geothermal systems (Brady's, Desert Peak, and Desert Queen). *Geothermal Resources Council Transactions*, **34**, 675-683.
[28] Faulds, J., Coolbaugh, M., Bouchot, V., Moek, I., &Oguz, K. (2010b). Characterizing structural controls of geothermal reservoirs in the Great Basin, USA, and Western Turkey: developing successful exploration strategies in extended terranes. In *World Geothermal Congress 2010* (pp. 11-p).
[29] Fedi, M., & Florio, G. (2001). Detection of potential field source boundaries by the enhanced horizontal derivative method. *Geophysical prospecting*, **49** (1), 40-58.
[30] Girdler, R. W. (Ed.). (2013). *East African Rifts* (No. 40). Elsevier. (Book on gravity and magnetic)
[31] Golden, M. (1978). *The Geology of the area east of silale, rift valley province, Kenya* (Doctoral dissertation, Royal Holloway, University of London).
[32] Hackman, B. D., Charsley, T. J., Key, R. M., & Wilkinson, A. F. (1990). The development of the East African Rift system in north-central Kenya. *Tectonophysics*, **184** (2), 189-211.
[33] Hautot, S., Tarits, P., Whaler, K., Le Gall, B., Tiercelin, J., Le Turdu, C., (2000), Deep structure of the Baringo Rift Basin (Central Kenya) from three-dimensional magnetotelluric imaging: Implications for rift evolution, *Geophysics*, **105** (23), 493-23,518
[34] Hinze, W. J. (2003). Bouguer reduction density, why 2.67?. *Geophysics*, **68** (5), 1559-1560.
[35] Hinze, W. J., Aiken, C., Brozena, J., Coakley, B., Dater, D., Flanagan, G., ...&Kucks, R. (2005). New standards for reducing gravity data: The North American gravity database. *Geophysics*, **70** (4), J25-J32.
[36] Hinze, W. J., Von Frese, R. R., &Saad, A. H. (2013). *Gravity and magnetic exploration: Principles, practices, and applications*. Cambridge University Press.
[37] Holden, E. J., Dentith, M., &Kovesi, P. (2008). Towards the automated analysis of regional aeromagnetic data to identify regions prospective for gold deposits. *Computers & Geosciences*, **34**(11), 1505-1513.
[38] Hsu, S.-K., J.-C. Sibuet, and C.-T. Shyu (1996), High-resolution detection of geologic boundaries of potential field anomalies: An enhanced analytic signal technique, *Geophysics* **61**(2), 373-386
[39] Kanda I.K. (editor), L. Ranks, E.K. Bett, J.K. Kipngok, M. Mutonga, B. Sosi, J. Gichira, R.M Mwakirani, I.J. Mboin, C. Ndongoli, L. Odundo, E. Ouko, H. Mwawasi, (2011), Paka Prospect: Investigations of its geothermal potential. *GDCInternal report.*
[40] Kearey, P., Brooks, M., & Hill, I. (2013). An introduction to geophysical exploration. *John Wiley & Sons.*
[41] Keating, P., and M. Pilkington (2004), Euler deconvolution of the analytic signal and its application to magnetic interpretation, *Geophys. Prospect*. **52**(3), 165-182

[42] Lagat J.k., (editor), P.O. Omenda J. Mungania, N.O. Mariita, J.M. Wambugu, K. Opondo, C.O. Ofwona, G. Mwawongo, B.M. Kubo, G. Wetangula, (2007), Geoscientific Evaluation of the Paka Geothermal Prospect, KenGen*Internal report.*

[43] Lagat, J. K. E. (2007). Hydrothermal alteration mineralogy in geothermal fields with case examples from Olkaria domes geothermal field, Kenya. *001045504*.

[44] Lichoro, C. M., Árnason, K., & Cumming, W. (2017). Resistivity imaging of geothermal resources in northern Kenya rift by joint 1D inversion of MT and TEM data. *Geothermics*, **68**, 20-32.

[45] Longo, L. M., De Ritis, R., Ventura, G., &Chiappini, M. (2016). Analysis of the Aeromagnetic Anomalies of the AucaMahuida Volcano, Patagonia, Argentina. *Pure and Applied Geophysics*, **173**(10-11), 3273-3290.

[46] Ma, G., Liu, C., & Huang, D. (2015). The removal of additional edges in the edge detection of potential field data. *Journal of Applied Geophysics*, **114**, 168-173

[47] MacLeod, I. N., Jones, K., & Dai, T. F. (1993). The 3-D analytic signal in the interpretation of total magnetic field data at low magnetic latitudes. *Exploration Geophysics*, **24**(3/4), 679-688.

[48] Mariani, P., Braitenberg, C., &Ussami, N. (2013). Explaining the thick crust in Paraná basin, Brazil, with satellite GOCE gravity observations. *Journal of South American Earth Sciences*, **45**, 209-223.

[49] Mariita, N. (2007). The gravity method. *Short Course II on a surface exploration of geothermal resources, Kenya*, 1-9.

[50] Mariita, N.O., (2003), An Integrated geophysical study of the northern Kenya rift crustal structure: Implications for geothermal energy prospecting in Menengai area, *Ph.D. dissertation, University of Texas at El Paso, USA*, page 1-188

[51] Mariita, N.O., and Keller, G.R., (2007), An integrated geophysical study of the northern Kenya rift, *Journal of African Earth Sciences*,**48**, 80-94

[52] Maucourant, S., Giammanco, S., Greco, F., Dorizon, S., & Del Negro, C. (2014). Geophysical and geochemical methods applied to investigate fissure-related hydrothermal systems in the summit area of Mt. Etna volcano (Italy). *Journal of Volcanology and geothermal research*, **280**, 111-125.

[53] Miller, C. A. (2017). *Volcanic architecture and unrest processes: Insights from static and time-varying potential field models* (Doctoral dissertation, Science: Department of Earth Sciences).

[54] Morley, C. K. (1999a). AAPG Studies in Geology# 44, Chapter 10: Aspects of Transfer Zone Geometry and Evolution in East African Rifts.

[55] Morley, C. K. (1999b). Patterns of displacement along large normal faults: implications for basin evolution and fault propagation, based on examples from East Africa. *AAPG Bulletin*, **83**(4), 613-634.

[56] Mulwa, J. K., & Mariita, N. O. (2015). Dyking processes in Arus-Bogoria geothermal prospect in Kenya revealed using gravity and microseismic data. In *37th New Zealand Geothermal Workshop: The next 10,000 Megawatts*. The University of Auckland, New Zealand Geothermal Association.

[57] Mulwa, J. K., Kimata, F., Suzuki, S., &Kuria, Z. N. (2014). The seismicity in Kenya (East Africa) for the period 1906–2010: A review. *Journal of African Earth Sciences*, **89**, 72-78.

[58] Mulwa, J., & Mariita, N. (2013). A comparative analysis of gravity and microseismic results from Arus-Bogoria geothermal prospect, Kenya. *Scholarly Journal of Scientific Research and Essay (SJSRE), ISSN*, 2315-6163.

[59] Mutonga, M. (2013). The Geology of Paka Volcano, and its Implication on Geothermal. *Geothermal Resources Council Transactions*, 431-436.

[60] Mwakirani. R.M., (2011), Resistivity structure of Paka geothermal prospect in Kenya, *report*, **26**, 605-633

[61] Narayan, S., Sahoo, S. D., Pal, S. K., Kumar, U., Pathak, V. K., Majumdar, T. J., &Chouhan, A. (2017). Delineation of structural features over a part of the Bay of Bengal using total and balanced horizontal derivative techniques. *Geocarto International*, **32**(4), 351-366.

[62] Njue, L. M. (2015). A geological model of Korosi geothermal prospect, Kenya. In *Proceedings World Geothermal Congress, Melbourne, Australia, 19–25 April 2015*.

[63] Nyakundi, E. R. (2017). Geophysical Investigation of Geothermal Potential of the Gilgil Area, Nakuru County, Kenya Using Gravity Method *(Doctoral dissertation, Kenyatta University).*

[64] Ochieng, L. (2014). Overview of geothermal surface exploration methods. *001374011*.

[65] Oldenburg, D.W.,and Pratt, D.A., 2007. Geophysical Inversion for Mineral Exploration: a Decade of Progress in Theory and Practice. The Leading Edge, 61-95.

[66] Omenda, P. (2014). The geology and geothermal activity of the East African Rift. *001374011*.

[67] Omenda, P. A. (1998). The geology and structural controls of the Olkaria geothermal system, Kenya. *Geothermics*, **27**(1), 55-74.

[68] Omenda, P., & Simiyu, S. (2015). Country update report for Kenya 2010–2014. *Proceedings World Geothermal*.

[69] Oruç, B. (2011). Edge detection and depth estimation using a tilt angle map from gravity gradient data of the Kozaklı-Central Anatolia Region, Turkey. *Pure and applied geophysics*, **168**(10), 1769-1780.

[70] Oruç, B., Sertçelik, I., Kafadar, Ö.,&Selim, H. H. (2013). Structural interpretation of the Erzurum Basin, eastern Turkey, using curvature gravity gradient tensor and gravity inversion of basement relief. *Journal of Applied Geophysics*, **88**, 105-113.

[71] Owens, L., Porras, E., Spielman, P., & Walsh, P. (2015). Updated Geologic and Geochemical Assessment of the Olkaria III Field Following Recent Expansion to 110MW. In *Fourtieth Workshop on Geothermal Reservoir Engineering Stanford University, Stanford, California, January 26*, **28**, p. 2015).

[72] Pal, S. K. (2009). A Geographical Information System based integrated study of remote sensing and

gravity data for geological appraisal of parts of Singhbhum-Orissa Craton, India [Ph.D. thesis]. *Kharagpur: Department of Geology and Geophysics, IIT Kharagpur*.

[73] Patlan, E., Velasco, A. A., Wamalwa, A., &Kaip, G. (2017) Seismic Zone at East Africa Rift: Insights into the Geothermal Potential.*Proceedings, 42nd Workshop on Geothermal Reservoir Engineering Stanford University, Stanford, California, February 13-15, 2017*

[74] Pawlowski, R. S. (1994). Green's equivalent-layer concept in gravity band-pass filter design. *Geophysics*, **59** (1), 69-76.

[75] Prodehl, C., Keller, G.R., Khan, M.A., (Eds), (1994), Crustal and Upper mantle structure of the Kenya Rift, *Tectonophysics*, **236**, 2-483

[76] Prodehl, C., Ritter, J., Mechie, J., Keller, G.R., Khan, M.A., Fuchs, K., Nyambok, I.O., Obel, J.D, (1997), The KRISP 94 Lithospheric investigation of southern Kenya-the experiments and their main results, In: Stress and stress release in the Lithosphere, *Tectonophysics*, **278**, 121-148

[77] Richarte, D., Lupari, M., Pesce, A., Nacif, S., &Gimenez, M. (2018). 3-D crustal-scale gravity model of the San Rafael Block and Payenia volcanic province in Mendoza, Argentina. *Geoscience Frontiers*, **9**(1), 239-248.

[78] Robertson, E. A. M., Biggs, J., Cashman, K. V., Floyd, M. A., &Vye-Brown, C. (2016). Influence of regional tectonics and pre-existing structures on the formation of elliptical calderas in the Kenyan Rift. *Geological Society, London, Special Publications*, **420**(1), 43-67

[79] Roest, W.R., J. Verhoef, and M. Pilkington (1992), Magnetic interpretation using 3-D analytic signal, *Geophysics*,**57**(1), 116-125

[80] Rosid, M. S., & Siregar, H. (2017, July). Determining fault structure using first horizontal derivative (FHD) and horizontal vertical diagonal maxima (HVDM) method: A comparative study. In *AIP Conference Proceedings*, **1862**(1), p. 030171. AIP Publishing.

[81] Roy, R., Benedicto, A., Grare, A., Béhaegel, M., Richard, Y., & Harrison, G. (2017). Three-dimensional gravity modeling applied to the exploration of uranium unconformity-related basement-hosted deposits: the Contact prospect case study, Kiggavik, northeast Thelon region (Nunavut, Canada). *Canadian Journal of Earth Sciences*, **54**(8), 869-882.

[82] Salem, A., Williams, S., Fairhead, D., Smith, R., &Ravat, D. (2007). Interpretation of magnetic data using tilt-angle derivatives. *Geophysics*, **73** (1), 1-10.

[83] Sceal, J. S. C., (1974), The geology of Paka volcano and the country to the east, Baringo District, Kenya, *unpublished Ph.D. thesis, University of London*

[84] Shako, L., & Wamalwa, A. (2014). GIS Applications in Heat Source Mapping in Menengai Geothermal Field. In *Proceedings of the 5th African Rift Geothermal Conference*.

[85] Simiyu, S. M., & Keller, G. R. (2000). Seismic monitoring of the Olkaria Geothermal area, Kenya Rift valley. *Journal of Volcanology and Geothermal Research*, **95**(1-4), 197-208.

[86] Simiyu, S. M., Omenda, P. A., Anthony, E. Y., & Keller, G. R. (1995). Geophysical and geological evidence for the occurrence of shallow magmatic intrusions in the Naivasha sub-basin of the Kenya Rift. *EOS Transactions of the AGU*, **76**, 257-258.

[87] Simiyu, S.M. and Keller G.R., (2001), An integrated geophysical analysis of the upper crust of the southern Kenya rift, *Geophysical journal international*, **147**,543-556

[88] Simiyu, S.M. and Keller, G.R., (1997), An integrated analysis of lithospheric structure across the East African plateau based on gravity anomalies and recent seismic studies, *Tectonophysics*, **278**, 291-313

[89] Simiyu, S.M., 1996. Integrated geophysical study of the crustal structure of the southern Kenya Rift. Ph.D. Dissertation, University Texas-El Paso, 240 pp.

[90] Sippel, J., Meeßen, C., Cacace, M., Mechie, J., Fishwick, S., Heine, C., ...&Strecker, M. R. (2017). The Kenya rift revisited: insights into lithospheric strength through data-driven 3-D gravity and thermal modeling. *Solid Earth*, **8**(1), 45-46.

[91] Smith, M., (1994), Stratigraphic and structural constraints on mechanisms of active rifting in the Gregory Rift, Kenya, *Tectonophysics*, **236**, 3-22

[92] Smith, M., Mosley, P.N., (1993), Crustal heterogeneity and basement influence on the development of the Kenya Rift, East Africa, *Tectonics*, **12**, 591-606

[93] Ström, T. (2018). A geophysical study of the Martinez area: Modelling and interpretation of primarily aeromagnetic data.

[94] Suzuki, K., Feely, M., & O'Reilly, C. (2001). Disturbance of the Re-Os chronometer of molybdenites from the late-Caledonian Galway Granite, Ireland, by hydrothermal fluid circulation. *Geochemical Journal*, **35**(1), 29-35.

[95] Swain, C.J. (1992), The Kenya rift axial gravity high: a re-interpretation, *Tectonophysics*, **204**, 59-70.

[96] Swain, C.J., Khan, M.A., Wilton, T.J., Maguire, P.K.H., Griffiths, D.H., (1981), Seismic and gravity surveys in the Lake Baringo-Tugen Hills area, Kenya rift valley, *Geological Society of London*, **138**, 93-102

[97] Tapponnier, P., & Molnar, P. (1977). Active faulting and tectonics in China. *Journal of Geophysical Research*, **82**(20), 2905-2930.

[98] Telford, W. M., Geldart, L. P., & Sheriff, R. E. (1990). *Applied geophysics* (Vol. **1**). Cambridge university press.

[99] Truckle, P. H. (1977). *The geology of the area to the south of Lokori, South Turkana, Kenya* (Doctoral dissertation, University of Leicester (United Kingdom)).

[100] Vaish, J., & Pal, S. K. (2015). Geological mapping of Jharia Coalfield, India using GRACE EGM2008 gravity data: a vertical derivative approach. *Geocarto International*, **30**(4), 388-401.

[101] Verduzco, B., J.D. Fairhead, C.M. Green, and C. MacKenzie (2004), New insights into magnetic derivatives for structural mapping, *The Leading Edge*, **23**, 116-119.

[102] Violay, M., Gibert, B., Mainprice, D., & Burg, J. P. (2015). Brittle versus ductile deformation as the main control of the deep fluid circulation in oceanic

crust. *Geophysical Research Letters*, **42**(8), 2767-2773.

[103] Wadge, G., Biggs, J., Lloyd, R., & Kendall, J. M. (2016). Historical volcanism and the state of stress in the East African Rift System. *Frontiers in Earth Science*, **4,** 86pg

[104] Walia, V., Lin, S. J., Fu, C. C., Yang, T. F., Hong, W. L., Wen, K. L., & Chen, C. H. (2010). Soil–gas monitoring: a tool for fault delineation studies along Hsinhua Fault (Tainan), Southern Taiwan. *Applied Geochemistry*, **25**(4), 602-607.

[105] Wamalwa, A. M., & Serpa, L. F. (2013). The investigation of the geothermal potential at the Silali volcano, Northern Kenya Rift, using electromagnetic data. *Geothermic*, **47**, 89-96.

[106] Wamalwa, R. N., Nyamai, C. M., Ambusso, W. J., Mulwa, J., & Waswa, A. K. (2016). Structural Controls on the Geochemistry and Output of the Wells in the Olkaria Geothermal Field of the Kenyan Rift Valley. *International Journal of Geosciences*, **7**(11), 1299.

[107] Waswa, A. K. (2017). Mapping of Hydrothermal Minerals Related to Geothermal Activities Using Remote Sensing and GIS: Case Study of Paka Volcano in Kenyan Rift Valley. *International Journal of Geosciences*, **8**(05), 711-725

[108] Wilks, M., Kendall, J. M., Nowacki, A., Biggs, J., Wookey, J., Birhanu, Y., ...&Bedada, T. (2017). Seismicity associated with magmatism, faulting and hydrothermal circulation at Aluto Volcano, Main Ethiopian Rift. *Journal of Volcanology and Geothermal Research*, **340**, 52-67.

[109] Wrage, J., Tardani, D., Reich, M., Daniele, L., Arancibia, G., Cembrano, J., ...& Pérez-Moreno, R. (2017). Geochemistry of thermal waters in the Southern Volcanic Zone, Chile–Implications for structural controls on geothermal fluid composition. *Chemical Geology*, **466**, 545-561.

[110] Yang, J., Latychev, K., & Edwards, R. N. (1998). Numerical computation of hydrothermal fluid circulation in fractured Earth structures. *Geophysical Journal International*, **135**(2), 627-649.

[111] Yuan, Y., & Yu, Q. (2015). Edge detection in potential-field gradient tensor data by use of improved horizontal analytical signal methods. *Pure and Applied Geophysics*, **172**(2), 461-472

Author Profile

Wafula Chembeni Peter, MSc Geophysics Student, Department of Physics, Egerton University, Egerton, Kenya

Sirma Chebet Ruth, MSc Geophysics Student, Department of Physics, Egerton University, Egerton, Kenya

Kirui Msk, PhD Physics L, Department of Physics, Egerton University, Egerton, Kenya